

Running title: Casp-14 in LADC

Caspase-14 is an anti-apoptotic protein targeting at apoptosis-inducing factor in lung adenocarcinomas

Hsin-Yuan Fang^{1,2}, Kuan-Chih Chow³, Ting-Chieh Chiang³, Min-Fa Hung³, Yi-Ting Hsiao³, Tze-Yi Lin⁴, I-Ping Chiang⁴, Chih-Yi Chen², Wen-Je Ko¹

¹Graduate Institute of Clinical Medicine, National Taiwan University, Taipei, Taiwan;

²Division of Thoracic Surgery, Department of Surgery, China Medical University Hospital, China Medical University, Taichung, Taiwan; ³Graduate Institute of Biomedical Sciences, National Chung Hsing University, Taichung, Taiwan; and ⁴Department of Pathology, China Medical University Hospital, China Medical University, Taichung, Taiwan

Abstract: word counts, 132

Text: 13 pages; word counts, 3584

Figures: 4

Tables: 2

Supplementary materials: 2 tables and 3 figures

Address for correspondence: Kuan-Chih Chow, Ph.D., Institute of Biomedical Sciences, National Chung Hsing University, 250 Kuo-Kuang Road, Taichung 40227, Taiwan. E-mail: kcchow@dragon.nchu.edu.tw; or Wen-Je Ko, MD, Graduate Institute of Clinical Medicine, National Taiwan University, 1 Jen Ai Road, Taipei 100, Taiwan. E-mail: kowj@ntu.edu.tw

E-mail address

Hsin-Yuan Fang, fanghy@mail.cmuh.org.tw

Kuan-Chih Chow, kcchow@dragon.nchu.edu.tw

Ting-Chieh Chiang, fin398@hotmail.com

Min-Fa Hung, minfahong@gmail.com

Yi-Ting Hsiao, vernaerin@yahoo.com.tw

Tze-Yi Lin, tylin.tw@msa.hinet.net

I-Ping Chiang, ipchiang@www.cmuh.org.tw

Chih-Yi Chen, micc@www.cmuh.org.tw

Wen-Je Ko, wenje@ha.mc.ntu.edu.tw

Abstract

Background: Using apoptosis-inducing factor protein as bait in a yeast hybrid assay to screen protein libraries, we identified three proteins that interacted with apoptosis-inducing factor: human homolog of yeast Rad23 protein A, microsomal glutathione S-transferase and caspase-14. In this study, we investigated the expression and function of caspase-14 in lung adenocarcinomas.

Results: Our results showed the monoclonal antibodies were specific to caspase-14, and that caspase-14 was highly expressed in lung adenocarcinomas. Overexpression of caspase-14 correlated with tumor stage, cell differentiation and lymphovascular involvement, suggesting that caspase-14 was associated with tumor cell growth and metastatic potential. *In vitro*, caspase-14 interacted with apoptosis-inducing factor, and silencing of caspase-14 expression reduced cisplatin resistance.

Conclusions: Our data suggest that caspase-14 is an anti-apoptotic protein targeting at apoptosis-inducing factor and increases cisplatin resistance in lung adenocarcinoma cells.

Keywords: caspase-14, apoptosis-inducing factor, cisplatin resistance, lung adenocarcinoma, anti-apoptosis

Abbreviations: AIF, apoptosis-inducing factor protein; CPD, cyclobutane pyrimidine dimers; EGFP, enhanced green fluorescent protein; GST, glutathione S-transferase; hHR23, human homolog of yeast Rad23 protein; LADC, lung adenocarcinoma; NTLT, non-tumor lung tissues; PCD, programmed cell death; UV, ultraviolet

Introduction

Programmed cell death (PCD) is a controlled process of tissue demolition that is imperative for regulating the development and tissue homeostasis in multicellular organisms [1]. Based on morphological and biochemical characteristics three types of PCD have been categorized [2-4]. However, only type I PCD, which is featured by nuclear events, e.g., DNA fragmentation, chromatin condensation and appearance of micronuclei, and cytoplasmic events, e.g., extensive membrane blebbing, phospholipid scrambling, loss of matrix attachment and cellular shrinkage, is mediated by apoptogenic proteins, such as apoptosis-inducing factor (AIF), cytochrome C (cyt C) and caspases [5]. AIF and cyt C are located in intermembranous space (IMS) of mitochondria. PCD, which is initiated *via* cyt C and activation of caspases, is called caspase-dependent apoptosis. On the other hand, PCD, which is initiated by nuclear translocation of AIF, but does not require caspase activation, is called caspase-independent apoptosis. Type II PCD and type III PCD are also initiated in a caspase-independent manner. Interestingly, mitochondria and dynamin-related protein 1 (DRP1), an 80-kDa GTPase which is involved in mitochondrial fission and anticancer drug-mediated cytotoxicity, are involved in all three types of programmed cell death [4,7,8].

Besides being an apoptogenic protein during programmed cell death, AIF is in fact an indispensable mitochondrial flavoprotein [9]. Upon exposure to genotoxic agents, e.g., cisplatin, adriamycin, staurosporine, camptothecin and etoposide, AIF is rapidly released from mitochondria and translocated to the nucleus to initiate degradation of poly(ADP-ribose) polymerase, DNA fragmentation, chromatin condensation and formation of micronuclei, the hallmarks of nuclear apoptosis [9-14]. However, AIF does not interact with karyopherins, the important nucleocytoplasmic shuttle [15]. We therefore propose that nuclear translocation of the protein may require vehicles other than karyopherins. Using full-length AIF protein as bait in a yeast hybrid assay to search libraries containing cytoplasmic and nuclear proteins,

we identified three proteins that interacted with AIF: human homolog of yeast Rad23 protein A (hHR23A) in the nuclear protein library, and hHR23A, microsomal glutathione S-transferase and caspase-14 in the cytoplasmic protein library (Table 1). As the shortest member of caspase family, caspase-14 is phylogenetically closest to caspase-2 (shared 26% amino acid identity). However, according to pathophysiological functions, caspase-14 is not able to be categorized into any of the three groups: cytokine activators, initiator or executioner caspases. Unlike the other caspases, the caspase-14 is not proteolytically processed at Asp residue in the linker region [1,16], but is cleaved between ¹⁵²Ile and ¹⁵³Lys in terminally differentiated keratinocytes [17]. Interestingly, knockout of caspase-14 gene increases epidermal storage of profilaggrin and ultraviolet (UV) B sensitivity, suggesting that caspase-14 plays a role in protein maturation of filaggrin [18], and possibly in DNA repair. Recently, overexpression of caspase-14 has been described in several of epithelial malignancies, indicating that caspase-14 could play a role in carcinogenesis and disease progression in cancer patients [19,20]. However, caspase-14 has not been studied in the lung adenocarcinoma, of which the incidence and mortality have increased dramatically in the last two decades in Taiwan [21]. Although cigarette smoking has been suggested being a key factor of disease progression and treatment failure [14], a portion of patients who do not respond well to the radiation- and chemotherapy in Taiwan are women and nonsmokers [22]. Treatment failures are major reasons for the high disease-related mortality. Since caspase-14 binds AIF, we thus hypothesize that caspase-14 may act as an anti-apoptotic marker by interfering AIF function and reduce drug sensitivity in cancer cells.

In this study, we examined the expression level of caspase-14 in lung adenocarcinoma (LADC) cells and pathological specimens. The correlation between caspase-14 expression and patient survival was evaluated statistically. Interaction between caspase-14 and AIF as well as the effect of caspase-14 on cell growth and drug resistance was characterized *in vitro*.

Materials and methods

Patients and tissue specimens

The patients in this study were from the same cohort used in the previous study [21]. Briefly, from January to December 2001, sera and tissue specimens were collected from 264 patients with newly diagnosed NSCLC. Samples from all patients, for whom at least one follow-up examination or death was documented, were pathologically confirmed NSCLC. Of the 264 patients, 107 were diagnosed as having lung ADC. The stage of the disease was classified according to the new international staging system for lung cancer [23]. The Medical Ethics Committee approved the protocol, and written informed consent was obtained from every patient before surgery. All patients had undergone surgical resection and radical N2 lymph node dissection. Tumor size, lymph node number, differentiation, vascular invasion and mitotic number were also evaluated. Patients with lymph node involvement or loco-regional recurrence received irradiation at the afflicted areas. Those with distant metastasis were treated with chemotherapy. After treatment, patients were routinely followed every 3 to 6 months in the outpatient department. Results from blood examination, biochemical studies, chest radiography, abdominal sonography, whole body bone scan and computerized tomography scans of chest that indicated any evidence of disease were interpreted as tumor recurrence and metastasis. The average age of the male patients ($n = 84$) was 60.6 ± 1.4 years and that of the female patients ($n = 23$) was 53.3 ± 1.3 years. Immunohistochemical staining was carried out using a single-blind procedure.

Reverse transcription-polymerase chain reaction (RT-PCR)

Following total RNA extraction and synthesis of the first-strand cDNA, an aliquot of cDNA was subjected to 35 cycles of PCR to determine the integrity of β -actin mRNA [14,21]. The cDNA used in the following RT-PCR was adjusted according to the quality and quantity of

β -actin mRNA. The primer sequences were selected by a web program, Primer3 at <http://frodo.wi.mit.edu/primer3>. For caspase-14, the primers are: Casp-14s: 5'-GAAATGAGCAATCCGCGGTCT-3' [sense primer, nts 46-66, NM_012114] and Casp-14a: 5'-CTACTGCAGATACAGCCGTTT-3' [antisense primer, nts 777-757].

Preparation of mouse antibodies

DNA sequence corresponding to full-length caspase-14 was amplified by primer sequences containing *Eco RI* (sense) and *Hind III* (antisense) restriction sites respectively. The primer sequences were *Casp-14s*: 5'-TCCGAAATTCATGAGCAATCCGCGGTCTTTG-3' (*Eco RI* site is underlined) and *Casp-14a*: 5'-GCAAAGCTTGCTACTGCAGATACAGCCGTTT-3' (*Hind III* site is underlined). The restriction fragment of caspase-14 was cloned into an expression vector pET-32b+ (Promega KK, Tokyo, Japan). Bacterial colony containing pET32+-caspase-14 was selected, and induced by isopropyl-beta-D-thiogalactopyranoside (IPTG) to mass-produce caspase-14. Recombinant protein was purified by a nickel-affinity column. Affinity-purified caspase-14 was used to immunize BALB/c mice, and sensitivity of antiserum (OD₄₀₅ > 0.3 at 1:6,000 dilutions) was measured by enzyme-linked immunosorbent assay (ELISA). Specificity of antibodies was determined by the appearance of a 35-kDa band in immunoblotting of lung cancer cell extract [24]. Monoclonal antibodies were produced by a hybridoma technique, and caspase-14-specific antibodies were screened by the methods mentioned above.

Immunoblotting analysis and immunocytochemistry

Total cell lysate was prepared by mixing 5×10^7 cells/100 μ l phosphate-buffered saline with equal volume of $2 \times$ loading buffer (50 mM Tris, pH 6.8, 150 mM NaCl, 1 mM disodium EDTA, 1 mM PMSF, 10% glycerol, 5% β -mercaptoethanol, 0.01% bromophenol blue and 1%

SDS). Electrophoresis was carried out in a 10% polyacrylamide gel with 4.5% stacking. Proteins were transferred to a nitrocellulose membrane after electrophoresis. The membrane was probed with specific antibodies. The signal was amplified by biotin-labeled goat anti-mouse IgG, and peroxidase-conjugated streptavidin. The protein was visualized by exposing the membrane to an X-Omat film (Eastman Kodak, Rochester, NY) with enhanced chemiluminescent reagent (NEN, Boston, MA). Immunocytochemical staining was performed by an immunoperoxidase method using labeled streptavidin-biotin complex (DAKO, LSAB2 System, Carpinteria, CA) [14,21]. For confocal immunofluorescence microscopy, the second antibodies contained fluorescence proteins.

Immunohistochemistry

Immunohistological staining was performed by an immunoperoxidase method [14,21]. Briefly, following removal of paraffin with xylene and absolute alcohol, antigen was retrieved by treating samples in boiling water for 10 minutes. Endogenous myeloperoxidase was inactivated with 3% H₂O₂ and 0.1% sodium azide at room temperature for 15 minutes. After incubation with monoclonal antibodies (1:100 dilutions) specific to caspase-14 at room temperature for two hours, specimens were treated with biotin-conjugated goat anti-mouse immunoglobulin, and then peroxidase-conjugated streptavidin. Chromogenic development was in 3-amino-9-ethylcarbazole. The slides were counterstained with 50% hematoxylin at RT for 45 seconds and the blue color was enhanced in running water for 20 minutes. The crimson precipitates were identified as positive staining. The non-tumor counterpart of the LADC tissue served as a negative control, and a section of gelatin-embedded H23 LADC cells was used as a positive control for each run of immunostaining.

Slide evaluation

In each pathological section, non-tumor lung tissue (NTLT) served as an internal negative control. Slides were evaluated by two independent pathologists blinded to the clinicopathological knowledge. The ImmunoReactive Scoring system was adapted for this study [25]. Briefly, a specimen was considered having strong signals when more than 50% of cancer cells were positively stained; intermediate, if 25-50% of the cells stained positive; weak, if less than 25% or more than 10% of the cells were positively stained; and negative, if less than 10% of the cells were positively stained. Cases with strong and intermediate caspase-14 signals were classified as Casp-14+, and those with weak or negative caspase-14 signals were classified as Casp-14-.

Cytotoxicity assay

Cells were seeded at 5000 cells/well 18 hr prior to challenge with various doses of cisplatin. The control group was treated with RPMI 1640. Following cell challenge for 48 hours, 10 μ l of WST-1 (BioVision, Mountain View, CA) was added and continued incubation for two hours. Percent survival of cells was quantified by comparing the number of viable cells in the treatment group with that in the control group. All procedures were performed in triplicate. This assay measures both replicating and static cells [14,21].

Statistical analysis

The relationship between caspase-14 expression and clinicopathological parameters was analyzed by Chi-Square test. Survival curves were plotted using the Kaplan-Meier estimator [26]. Statistical difference in survival among different groups was compared by the log rank test (between Casp-14+ and Casp-14-groups) [27]. Statistical analysis was performed using GraphPad Prism5 statistical software (San Diego, CA). Statistical significance was set at p value < 0.05 .

Results

Expression of caspase-14 in LADC cells determined by RT-PCR

Expression of caspase-14 was examined by RT-PCR in one HeLa and in eight lung cancer cell lines. Caspase-14 was detected in all cell lines (Fig. 1). Following sequence analysis (by Mission Biotech, www.missionbio.com.tw, Taipei, Taiwan, on ABI PRISM, model 3730), nucleotide sequence of cDNA fragments from the nine cell lines matched that of caspase-14: NM_012114, *Homo sapiens* caspase-14, apoptosis-related cysteine peptidase (Casp-14), mRNA, identities = 775/777 (99.7%). Two point mutation sites were identified: 109cta → 109gta (Leu21Val) in three of nine samples and 724aaa → 724gaa (Lys226Glu) in six of nine samples (The sequence was presented in GenBank, EU262664.1; and Supplementary Fig. S1). Interestingly, mutation in these two positions increased the probability of protein nuclear localization when protein sequences were analyzed by a PSORT II prediction program (<http://psort.ims.u-tokyo.ac.jp/>) (Supplementary Table S1). However, no nuclear localization signal (NLS) was identified in either wild-type or the mutated sequences using a web prediction program (<http://www.rostlab.org/services/predictNLS/>).

Characterization of monoclonal antibodies to caspase-14 and expression of caspase-14 in LADC cell lines

Specificity of monoclonal antibodies was determined by an immunoblotting of H23 cell lysate. A 35-kDa protein corresponding to the anticipated molecular mass of caspase-14 was recognized [24]. For confirming the specificity of the antibodies, we cloned caspase-14 gene into a mammalian vector (pcDNA3.1-casp-14) or into a pEGFP-N1 vector, which carried an enhanced green fluorescent protein (EGFP) gene (pEGFP-casp-14). As shown in Fig. 2A, our monoclonal antibodies recognized the anticipated protein bands in both transfectants. Using immunoblotting, expression of caspase-14 was detected in H23, H226, H838, H2009 and

H2087 (Fig. 2B). Immunocytochemistry and fluorescence microscopy showed that caspase-14 was abundantly present in the cytoplasm or in the nuclei depending upon the cell type (Fig. 2C & 2D). However, unlike DRP1 [28], caspase-14 signal was not present in the nucleoli. In HeLa cells transfected with pEGFP-casp-14, the EGFP-casp-14 was detected in cytoplasm of the resting cells and in nuclei of the replicating cells (Fig. 2E). Likewise, nucleolus was devoid of EGFP-casp-14. Sub-organelle fractionation showed that caspase-14 was detected in both cytoplasm and nucleus (Fig. 2F), indicating that the nuclear caspase-14 signals were genuine, not an artifact of immunocytochemistry or fluorescence microscopy. No obvious differentiation was detected in HeLa or LADC cells with enforced expression of caspase-14.

Increased caspase-14 expression reduces cisplatin sensitivity, possibly *via* interaction with AIF

Interestingly, A549 cells that were transfected either with pcDNA3.1-casp-14 or with pEGFP-casp-14 were more resistant to cisplatin (Fig. 3A). Moreover, using siRNA to knockdown casp-14 (casp-14kd)-specific expression in H23 cells (Fig. 3B1) significantly reduced cisplatin resistance (Fig. 3B2), supporting our anticipations that expression of caspase-14 might increase drug resistance, possibly, by binding to AIF.

As noted previously, using yeast two-hybrid assays, we had identified that AIF reacted with caspase-14 in the cytoplasmic protein library. Antibodies specific to caspase-14 precipitated both caspase-14 and AIF from the whole cell lysate (Fig. 3C). Using deletion mutants to determine the specific binding segment of caspase-14, which was inserted into pGEX-4T-1/*GST*, *GST*-casp-14 and *GST*-casp-14-N152, but not *GST*-casp-14- Δ N152, could pull down AIF (Fig. 3D). *GST*-casp-14-N152 contained amino acids 1-152 of the human caspase-14, including the two hydrophobic segments (Supplementary Fig. S2) [24].

GST-casp-14- Δ N152 contained amino acids 153-242 of the human caspase-14 (deletion of the N-terminal 152 amino acid residues). Results of immunoprecipitation and protein pull-down assays confirmed our data of the yeast two hybrid assays that caspase-14 interacted with AIF.

Expression of caspase-14 in LADC correlated with increase of tumor recurrence and decrease of patient's survival

Using immunoblotting, while only the 35-kDa caspase-14 was detected in the non-tumor lung tissues (NLT), two caspase-14-positive bands, 35- and 37-kDa, were identified in the LADC specimens (Fig. 4A). Although a 37-kDa protein was detected in pathological specimens, it was not detected in the lung cancer cell lines. We were uncertain whether the 37-kDa band represented a phosphorylated caspase-14. To resolve this issue, tissue lysate of LADC was treated with calf intestinal alkaline phosphatase (CIP) before immunoblotting. The assay revealed a clear reduction in signals of the 37-kDa protein band (Fig. 4B). These results suggested that the 37-kDa protein could be phosphorylated caspase-14. Using a NetPhos program (<http://www.cbs.dtu.dk/services/NetPhos/>) to predict for phosphorylation sites, and using a NetPhosK program (<http://www.cbs.dtu.dk/services/NetPhosK/>) to predict for specific kinase in eukaryotic proteins, the results suggested that the most probable kinase was protein kinase C (PKC) at ²⁰¹Thr (Supplementary Table S2). However, no LADC cell line, which expresses the 37-kDa caspase-14, is available for study.

We tested our antibodies on psoriatic lesions (Supplementary Fig. S3), and the results were identical to what was obtained by Lippens *et al* [24], and immunohistochemistry detected caspase-14 in 88 (82.2%) of LADC pathological samples. The signal was mainly located in the cancer cells (Fig. 4C1), and in 80 (90.9%) of the pathological specimens the caspase-14 was identified in the nuclei (Fig. 4C2). However, the caspase-14 was not detected

in the NTLT (Fig. 4C3). Caspase-14 expression was also detected in 83.9% (47/56) of metastatic lymph nodes (data not shown). Statistical analysis showed that overexpression of caspase-14 in tumors correlated with tumor stage, cigarette smoking, cell differentiation and lymphovascular involvement (Table 2), suggesting that expression of caspase-14 was associated with tumor cell growth and metastatic potential of LADC cells. Interestingly, among the 88 patients who had high levels of caspase-14, 38 (43.2%) patients had tumor recurrence during follow-up examination. Among the 19 patients who had low levels of caspase-14, four had tumor recurrence (21.0%). All 42 patients who had recurrence developed tumors within 24 months after operation. The risk of recurrence for patients with high levels of caspase-14 was 2.31-fold higher than that for patients with low levels of caspase-14 ($p = 0.029$). Survival of patients with low caspase-14 levels was significantly better than that of patients with high caspase-14 levels (Fig. 4D1). The hazard ratio between these two groups was 2.323, and the difference in cumulative survival was significant ($p = 0.0022$). Multivariate analysis, however, did not show a significant statistical difference in caspase-14 expression between the two groups ($p = 0.0821$). When Casp-14+ group was subcategorized into nucleus-positive (nCasp-14+) and cytoplasm-positive (cytCasp-14+) groups, though a significant difference was found in the survival among the three groups ($p = 0.0302$), no significant difference was found between the nCasp-14+ and the cytCasp-14+ groups ($p = 0.47$) or that between the Casp-14- and the cytCasp-14+ groups ($p = 0.147$) (Fig. 4D2). The outcome could be due to the low sample number of cytoplasm-positive cases.

Discussion

The data presented above showed that expression of caspase-14 was frequently detected in pathological specimens of LADC. Moreover, caspase-14 expression significantly correlated with higher incidence of the early tumor recurrence and the increased drug resistance, which ultimately reflected in the poor survival. *In vitro*, caspase-14 binds the apoptosis-inducing factor (AIF), and the increased caspase-14 level correlates with reduced cisplatin sensitivity. These results suggested that caspase-14 could be an anti-apoptotic protein targeting at AIF in LADC cells.

Caspase and AIF have in recent years emerged as novel targets for anticancer drugs, including cisplatin, adriamycin, camptothecin and etoposide [3,14]. Current evidence suggests that drugs induce destabilization of mitochondrial membrane integrity, procaspase activation and nuclear translocation of AIF, which provokes DNA fragmentation, micronuclei formation and cell death [10]. Maintaining mitochondrial membrane integrity or interfering caspase activation as well as nuclear translocation of AIF could therefore alleviate drug-induced apoptosis. As noted above, using AIF as bait in a yeast two hybrid assay, we identified microsomal GST, hHR23A and caspase-14 in the protein library. As noted above that unlike the other caspases, caspase-14 is not cleaved at Asp residue of the linker region when cells were exposed to genotoxic stress. Moreover, using immunoprecipitation and protein pull-down assays, we showed that AIF interacts with caspase-14. By demonstrating that enforced caspase-14 expression decreases cisplatin-mediated cell killing, and silencing of caspase-14 expression increases cisplatin sensitivity, our data indicate that caspase-14 influences drug-related cell death, and suggest that the cytoprotection may possibly be *via* interference of AIF nuclear translocation.

In addition to AIF, nuclear level of other apoptosis-associated mitochondrial proteins, such as apoptotic protease activating factor 1 (Apaf-1), B cell lymphoma protein 2 (Bcl-2),

BH3-interacting death domain protein (BID), and Bcl-2 nineteen kilodalton interacting protein 3 (BNIP3) increases following genotoxic stresses, including UV irradiation, ionizing radiation and chemotherapeutics [29-32]. Moreover, these proteins are indeed “located in the nucleus” when cells have been exposed to genotoxic stress. Recent studies show that when these proteins are present in the nuclei, they are involved in the cell cycle progression and DNA repair, the processes that are mediated by p53, checkpoint (Chk)-1, Chk-2, ataxia telangiectasia mutated (ATM) as well as ATM and rad3-related (ATR) kinases [33]. Nuclear presence of these proteins increases genomic instability as well as resistance to irradiation and anticancer drugs [32,34], suggesting that the nuclear presence of these proteins is vital for the cell survival.

In fact, nuclear caspase-14 has been detected in the stratum spinosum of normal skin, psoriatic lesions and epithelial malignancies [19,20,24]. However, caspase-14 is not detected in basal and cornified layers of normal skin or in basal layer and parakeratotic abrasion of psoriasis. Since skin cells in basal layer and parakeratotic abrasion are undifferentiated cells, the results suggested that the protein could be involved in the differentiation of squamous cells [18,24]. The role of nuclear caspase-14 in cell differentiation, however, was not investigated. By showing that knockout of caspase-14 gene increases UVB sensitivity, Denecker *et al.* suggest that caspase-14 is essential for reducing dermal accumulation of the cyclobutane pyrimidine dimers (CPD), and for increasing p53-related cell survival [18]. Involvement of caspase-14 in these nuclear events, nonetheless, was not clearly elucidated. It is worth noting that following UV damage xeroderma pigmentosum complementation group C (XPC) protein and human homolog of yeast Rad23 protein B (hHR23B) are promptly recruited to the nucleus [35,36]. Inside the nucleus, hHR23B increases p53 accumulation and inhibits cell cycle progression, while XPC accelerates DNA repair and reduces DNA damage-associated apoptosis. Collaboration between XPC and hHR23B renders

cytoreistance to chemotherapeutics and irradiation [35]. A recent report showed that increased nuclear level of phosphorylated DRP1, which was accompanied by nuclear accumulation of hHR23A under hypoxic condition, was vital for protection of nucleoli and reduction of cisplatin sensitivity [28]. Interestingly, hHR23A binds caspase-14 as well (Supplementary Fig. S4). In an ongoing study, we are examining the role of hHR23A in the nuclear translocation of caspase-14. Taken together, our results clearly show that caspase-14, either cytoplasmic or nuclear, plays an imperative role in protecting cells from genotoxic damages, possibly by interfering nuclear translocation of AIF and binding of AIF to the genomic DNA. The essence of nuclear caspase-14 is yet to be determined.

Interestingly, oxidative stress increases nuclear translocation of focal adhesion kinase (FAK), an integrin- and hepatocyte growth factor (HGF)-associated tyrosine kinase which is normally located on plasma membrane, to modulate muscle differentiation as well [37]. Knockdown of FAK expression increased AIF expression and reduced cisplatin resistance of mouse embryonic fibroblasts [14,21,39]. These results corresponded well with our current findings, indicating that under unfavorable growth conditions, such as nutrient depletion or hypoxia, the cells might initiate emergency nuclear transport of vital proteins, such as FAK, DRP1 and caspase-14, to protect genomic DNA as well as to activate certain gene expression [14,21,28,37,39]. The nuclear events, however, are yet to be determined.

In conclusion, immunohistochemistry revealed abundant expression of caspase-14 in lung adenocarcinomas. Pathological results show that caspase-14 expression is associated with poor prognosis. *In vitro*, expression of caspase-14 increased cisplatin resistance in LADC cells. By showing that caspase-14 and AIF interact with each other, and that silencing of caspase-14 decreased cisplatin resistance, our results suggest that caspase-14 may play an important role in interfering nuclear function of AIF and increase drug resistance of LADC cells.

Acknowledgments

RNAi for silencing caspase-14 gene expression was obtained from the National RNAi Core Facility in the Institute of Molecular Biology/Genomic Research Center, Academia Sinica, Taipei, Taiwan, supported by the National Research Program for Genomic Medicine Grants of NSC (NSC 97-3112-B-001-016). This study was supported in part by the Comprehensive Academic Promotion Projects (NCHU 985005, from Department of Education, Executive Yuan, Republic of China, to K.C. Chow).

References

1. Taylor RC, Cullen SP, Martin SJ: Apoptosis: controlled demolition at the cellular level. *Nat Rev Mol Cell Biol* 2008, 9: 231-241.
2. Clarke PG: Developmental cell death: morphological diversity and multiple mechanisms. *Anat Embryol* 1990, 181:195-213.
3. Gozuacik D, Kimchi A: Autophagy as a cell death and tumor suppressor mechanism. *Oncogene* 2004, 23: 2891-2906.
4. Bras M, Yuste VJ, Roué G, Barbier S, Sancho P, Virely C, Rubio M, Baudet S, Esquerda JE, Merle-Béral H, Sarfati M, Susin SA: Drp1 mediates caspase-independent type III cell death in normal and leukemic cells. *Mol Cell Biol* 2007, 27: 7073-7088.
5. Lorenzo HK, Susin SA: Mitochondrial effectors in caspase-independent cell death. *FEBS Lett* 2004, 557: 14-20.
6. Jaattela M, Tschopp J: Caspase-independent cell death in T lymphocytes. *Nat Immunol* 2003, 4: 416-423.
7. Frank S, Gaume B, Bergmann-Leitner ES, Leitner WW, Robert EG, Catez F, Smith CL, Youle RJ: The role of dynamin-related protein 1, a mediator of mitochondrial fission, in apoptosis. *Dev Cell* 2001, 1: 515-525.
8. Barsoum MJ, Yuan H, Gerencser AA, Liot G, Kushnareva Y, Gräber S, Kovacs I, Lee WD, Waggoner J, Cui J, White AD, Bossy B, Martinou JC, Youle RJ, Lipton SA, Ellisman MH, Perkins GA, Bossy-Wetzler E: Nitric oxide-induced mitochondrial fission is regulated by dynamin-related GTPases in neurons. *EMBO J* 2006, 25: 3900-3911.
9. Susin SA, Lorenzo HK, Zamzami N, Marzo I, Snow BE, Brothers GM, Mangion J, Jacotot E, Costantini P, Loeffler M, Larochette N, Goodlett DR, Aebersold R, Siderovski DP, Penninger JM, Kroemer G: Molecular characterization of mitochondrial apoptosis-inducing factor. *Nature* 1999, 397: 441-446.

10. Daugas E, Susin SA, Zamzami N, Ferri KF, Irinopoulou T, Larochette N, Prévost MC, Leber B, Andrews D, Penninger J, Kroemer G: Mitochondrio-nuclear translocation of AIF in apoptosis and necrosis. *FASEB J* 2000, 14: 729-739.
11. Arnoult A, Gaume B, Karbowski M, Sharpe JC, Cecconi F, Youle RJ: Mitochondrial release of AIF and EndoG requires caspase activation downstream of Bax/Bak-mediated permeabilization. *EMBO J* 2003, 22: 4385-4399.
12. Wu J, Harris NL, Inge TH: Nuclear factor-kappa B and apoptosis inducing factor activation by doxorubicin analog WP744 in SH-SY5Y neuroblastoma cells. *J Surg Res* 2004, 122: 231-239.
13. Rodríguez-Hernández A, Brea-Calvo G, Fernández-Ayala DJ, Cordero M, Navas P, Sánchez-Alcázar JA: Nuclear caspase-3 and caspase-7 activation, and poly(ADP-ribose) polymerase cleavage are early events in camptothecin-induced apoptosis. *Apoptosis* 2006, 11: 131-139.
14. Chen JT, Huang CY, Chiang YY, Chen WH, Chiou SH, Chen CY, Chow KC: HGF increases cisplatin resistance via down-regulation of AIF in lung cancer cells. *Am J Respir Cell Mol Biol* 2008, 38: 559-565.
15. Chook YM, Blobel G: Karyopherins and nuclear import. *Curr Opin Struct Biol* 2001, 11:703-715.
16. Van de Craen M, Van Loo G, Pype S, Van Crielinge W, Van den brande I, Molemans F, Fiers W, Declercq W, Vandenaabeele P: Identification of a new caspase homologue: caspase-14. *Cell Death Differ* 1998, 5: 838-846.
17. Chien AJ, Presland RB, Kuechle MK: Processing of native caspase-14 occurs at an atypical cleavage site in normal epidermal differentiation. *Biochem Biophys Res Commun* 2002, 296: 911-917.

18. Denecker G, Hoste E, Gilbert B, Hochepped T, Ovaere P, Lippens S, Van den Broecke C, Van Damme P, D'Herde K, Hachem JP, Borgonie G, Presland RB, Schoonjans L, Libert C, Vandekerckhove J, Gevaert K, Vandenabeele P, Declercq W: Caspase-14 protects against epidermal UVB photodamage and water loss. *Nat Cell Biol* 2007, 9: 666-674.
19. Koenig U, Sommergruber W, Lippens S: Aberrant expression of caspase-14 in epithelial tumors. *Biochem Biophys Res Commun* 2005, 335: 309-313.
20. Krajewska M, Kim H, Shin E, Kennedy S, Duffy MJ, Wong YF, Marr D, Mikolajczyk J, Shabaik A, Meinhold-Heerlein I, Huang X, Banares S, Hedayat H, Reed JC, Krajewski S: Tumor-associated alterations in caspase-14 expression in epithelial malignancies. *Clin Cancer Res* 2005, 11: 5462-5471.
21. Chen JT, Lin TS, Chow KC, Huang HH, Chiou SH, Chiang SF, Chen HC, Chuang TL, Lin TY, Chen CY: Cigarette smoking induces overexpression of HGF in type II pneumocytes and lung cancer cells. *Am J Respir Cell Mol Biol* 2006, 34: 264-273.
22. Brownson RC, Alavanja MC, Hock ET, Loy TS: Passive smoking and lung cancer in nonsmoking women. *Am J Public Health* 1992, 82: 1525-1530.
23. Detterbeck FC, Boffa DJ, Tanoue LT. The new lung cancer staging system. *Chest* 2009, 136: 260-271.
24. Lippens S, Kockx M, Knaapen M, Mortier L, Polakowska R, Verheyen A, Garmyn M, Zwijsen A, Formstecher P, Huylebroeck D, Vandenabeele P, Declercq W: Epidermal differentiation does not involve the pro-apoptotic executioner caspases, but is associated with caspase-14 induction and processing. *Cell Death Differ* 2000, 7: 1218-1224.
25. Remmele W, Schicketanz KH: Immunohistochemical determination of estrogen and progesterone receptor content in human breast cancer. Computer-assisted image analysis (QIC score) vs. subjective grading (IRS). *Pathol Res Pract* 1993, 189: 862-866.
26. Kaplan EL, Meier P: Nonparametric estimation from incomplete observations. *J Am Stat*

- Assoc 1958, 53: 457-481.
27. Mantel N: Evaluation of survival data and two new rank order statistics arising in its consideration. *Cancer Chemother Rep* 1966, 50: 163-170.
 28. Chiang YY, Chen SL, Hsiao YT, Huang CH, Lin TY, Chiang IP, Hsu WH, Chow KC.: Nuclear expression of dynamin-related protein 1 in lung adenocarcinomas. *Mod Pathol* 2009, 22: 1139-1150.
 29. Kaminer I, Sarig RH, Zaltsman Y, Niv H, Oberkovitz G, Regev L, Haimovich G, Lerenthal Y, Marcellus RC, Gross A: Proapoptotic BID is an ATM effector in the DNA-damage response. *Cell* 2005, 122: 593-603.
 30. Zinkel SS, Hurov KE, Ong C, Abtahi FM, Gross A, Korsmeyer SJ: A role for proapoptotic BID in the DNA-damage response. *Cell* 2005, 122: 579-591.
 31. Burton TR, Henson ES, Baijal P, Eisenstat DD, Gibson SB: The pro-cell death Bcl-2 family member, BNIP3, is localized to the nucleus of human glial cells: Implications for glioblastoma multiforme tumor cell survival under hypoxia. *Int J Cancer* 2006, 118: 1660-1669.
 32. Zermati Y, Mouhamad S, Stergiou L, Besse B, Galluzzi L, Boehrer S, Pauleau AL, Rosselli F, D'Amelio M, Amendola R, Castedo M, Hengartner M, Soria JC, Cecconi F, Kroemer G: Nonapoptotic role for Apaf-1 in the DNA damage checkpoint. *Mol Cell* 2007, 28: 624-637.
 33. Bartek J, Bartkova J, Lukas J: DNA damage signalling guards against activated oncogenes and tumour progression. *Oncogene* 2007, 26: 7773-7779.
 34. Wang Q, Gao F, May WS, Zhang Y, Flagg T, Deng X: Bcl2 negatively regulates DNA double-strand-break repair through a nonhomologous end-joining pathway. *Mol Cell* 2008, 29: 488-498.
 35. Kaur M, Pop M, Shi D, Brignone C, Grossman SR: hHR23B is required for

- genotoxic-specific activation of p53 and apoptosis. *Oncogene* 2007, 26: 1231-1237.
36. Dominguez-Brauer C, Chen YJ, Brauer PM, Pimkina J, Raychaudhuri P: ARF stimulates XPC to trigger nucleotide excision repair by regulating the repressor complex of E2F4. *EMBO Rep* 2009, 10: 1036-1042.
 37. Luo SW, Zhang C, Zhang B, Kim CH, Qiu YZ, Du QS, Mei L, Xiong WC: Regulation of heterochromatin remodeling and myogenin expression during muscle differentiation by FAK interaction with MBD2. *EMBO J* 2009, 28: 2568-2582.
 38. Lim ST, Chen XL, Lim Y, Hanson DA, Vo TT, Howerton K, Larocque N, Fisher SJ, Schlaepfer DD, Ilic D: Nuclear FAK promotes cell proliferation and survival through FERM-enhanced p53 degradation. *Mol Cell* 2008, 29: 9-22.
 39. Zhou M, Zhao Y, Ding Y, Liu H, Liu Z, Fodstad O, Riker AI, Kamarajugadda S, Lu J, Owen LB, Ledoux SP, Tan M: Warburg effect in chemosensitivity: Targeting lactate dehydrogenase-A re-sensitizes Taxol-resistant cancer cells to Taxol. *Mol Cancer* 2010, 9:33. [Epub ahead of print]

Figure legends

Fig. 1 Expression of caspase detected by RT-PCR in lung adenocarcinoma cells.

Expression of β -actin was used as a monitoring standard for the relative expression ratio of caspase-14 mRNA.

Fig. 2 Characterization of monoclonal antibodies to caspase-14. **(A)** Immunoblotting revealed that monoclonal antibodies raised against recombinant caspase-14 recognized a 35-kDa protein band in whole cell lysate from H23 cells or pcDNA3.1-casp-14 transfected A549 cells. In pEGFP-casp-14 transfected A549 cells, the protein recognized is 55-kDa. **(B)** Using immunoblotting, expression of caspase-14 was detected in H23, H226, H838, H2009 and H2087 cells. **(C)** Immunocytochemical staining showed that caspase-14 was abundantly present in the cytoplasm and in the nucleus (arrows). **(D)** Confocal immunofluorescence microscopy of H838 and H1437 cells. Caspase-14 was detected by specific monoclonal antibodies labeled with fluorescein isothiocyanate (FITC). Nuclei were stained with fluorescent dye 4', 6-diamidino-2-phenylindole (DAPI). A merged image of the first and the second columns confirms that caspase-14 is located in the nucleus. **(E)** In pEGFP-casp-14 transfected HeLa cells, the fluorescence protein was detected in the cytoplasm of resting cells and in the nuclei of replicating cells (white arrows) by a fluorescence microscopy. Nucleolus was devoid of pEGFP-casp-14 (white arrowhead). **(F)** Antibodies specific to caspase-14 recognized the protein both in the cytoplasmic and nuclear fractions as determined by an immunoblotting.

Fig. 3 Effect of caspase-14 expression on cisplatin cytotoxicity. **(A)** Enforced expression of caspase-14, either transfected with pcDNA3.1-casp-14 (○) or with pEGFP-casp-14 (△), increased cisplatin cytotoxicity in A549 cells (□). **(B)** Reduction of caspase-14 expression

increased cisplatin sensitivity. **(B1)** Using siRNA could reduce about 80% of caspase-14 expression in H23 cells [knockdown casp-14 (casp-14^{kd})-specific expression]. **(B2)** Compared to the control H23 cells (●), casp-14^{kd} cells (○) are significantly more sensitive to cisplatin. **(C)** Caspase-14 interacts with AIF. Monoclonal antibodies specific to caspase-14 precipitated caspase-14 (the left panel) and AIF (the right panel) from the whole cell lysate of H23 by protein G sepharoseTM. **(D)** GST-pull down assay to determine the interaction between caspase-14 and AIF. Full-length and partial fragments of caspase-14 were inserted into pGEX-4T-1/*GST* (upper panel). GST-casp-14 contained the full-length of caspase-14 gene, while deletion mutants contained only segments of caspase-14, i.e., GST-casp-14-N152 contained amino acids 1-152, and GST-casp-14-ΔN152 contained amino acids 153-242 (deletion of the N-terminal 152 amino acid residues) of the human caspase-14 gene (central panel). Only GST-casp-14 and GST-casp-14-N152, but not GST-casp-14-ΔN152, could pull down AIF (bottom panel) as determined by an immunoblotting.

Fig. 4 Correlation between caspase-14 expression and survival in patients with LADC.

(A) Expression of caspase-14 was determined by immunoblotting. Expression of β-actin was used as a monitoring standard for the relative expression of caspase-14. Interestingly, while only the 35-kDa caspase-14 was detected in the non-tumor lung tissues (NLT), two caspase-14-positive bands, 35- and 37-kDa, were identified in the LADC specimens. The 37-kDa protein was not detected in the lung cancer cell lines. N: NLT, T: tumor fraction of surgical resections. **(B)** Pooled tissue lysate (75 μg) of LADC, which was collected by using a buffer containing non-ionic NP-40, was treated with calf intestinal alkaline phosphatase (CIP) before immunoblotting. Addition of CIP clearly reduced signals of the 37-kDa protein band. The results suggested that the 37-kDa protein could be a phosphorylated caspase-14. **(C)** Representative examples of caspase-14 expression in pathological specimens as detected by

immunohistochemical staining (as crimson precipitates). Expression of caspase-14 was detected in (C1) the cytoplasm and (C2) the nucleus of LADC tumor cells, but not (C3) in the NTLT. (D) Comparison of Kaplan-Meier product limit estimates of survival analysis in patients with LADC. **D1:** Patients were divided into two groups based on expression of caspase-14. Survival difference between the two groups was compared by a log rank test. $p = 0.0022$; **D2:** To determine the effect of nuclear caspase-14 on survival, the Casp-14⁺ group was subcategorized into nucleus-positive (nCasp-14⁺) and cytoplasm-positive (cytCasp-14⁺) groups. Although a significant difference was found in the patient's survival among the three (nCasp-14⁺, cytCasp-14⁺ and Casp-14⁻) groups by a logrank test for trend ($p = 0.0302$), no significant difference was detected between nCasp-14⁺ and cytCasp-14⁺ groups ($p = 0.47$) or that between Casp-14⁻ and cytCasp-14⁺ groups ($p = 0.147$).

Table 1

Table 1 Proteins that interact with AIF in libraries containing cytoplasmic (Modules LPap002, LPap003 and LPap005, Level Biotechnology Inc., Taipei, Taiwan) or nuclear (Module LPtf010) proteins, which are identified by using AIF as the bait in a yeast two-hybrid assay.

Module	Location	Acc. No.	Gene name	Growth selection		X-gal assay	
				1st	repeat	1st	repeat
LPtf005	E8, E9	NM_005053	Rad23 (<i>S. cerevisiae</i>) homolog A	+++	+++	+++	+++
LPtf005	F2, F3	NM_020300	Microsomal glutathione <i>S</i> -transferase 1 (MGST1)	+++	+++	+++	+++
LPtf005	F10, F11	NM_012114	Caspase-14	+++	+++	+++	+++
Module	Location	Acc. No.	Gene name	Growth selection		X-gal assay	
LPtf010	E10, E11	NM_005053	Rad23 (<i>S. cerevisiae</i>) homolog A	+++		+++	

Table 2 Correlation of casp-14 expression with clinicopathological parameters in patients with LADC

Parameter	Expression of casp-14		<i>p</i> value	
	High (n = 88)	Low (n = 19)	Univariate	Multivariate
Gender				
Male (n = 84)	72	12	0.073 [†]	0.169
Female (n = 23)	16	7		
Cigarette Smoking				
Smoker (n = 78)	68	10	0.028 [†]	0.087
Non-smoker (n = 29)	20	9		
Stage				
I (n = 26)	18	8	0.002 [‡]	0.018
II (n = 31)	22	9		
III (n = 50)	48	2		
Cell differentiation				
Well (n = 17)	10	7	0.019 [‡]	0.076
Moderate (n = 60)	51	9		
Poor (n = 30)	27	3		
Lymphovascular invasion				
Positive (n = 81)	69	12	0.029 [†]	0.092
Negative (n = 26)	19	7		

[†]Two-sided *p* value determined by χ^2 test

[‡]Two-sided *p* value determined by Fisher's exact test

H23 H125 H226 H838 H1437 H2009 H2087 A549 HeLa

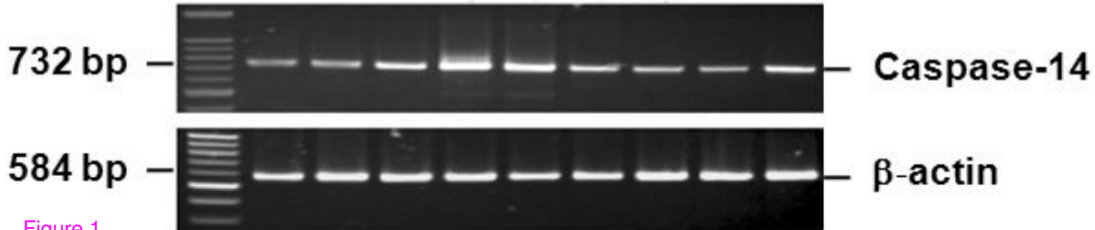


Figure 1

Control
pcDNA3.1-casp-14
pEGFP-casp-14

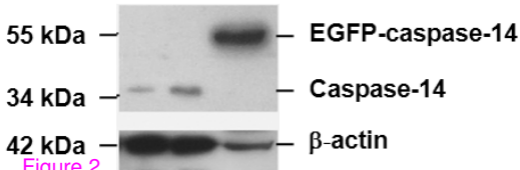


Figure 2

H23 H2226 H8338 H1437 H2009 H2087 A549 HeLa

35 kDa



Caspase-14

42 kDa



β-actin

Figure 3

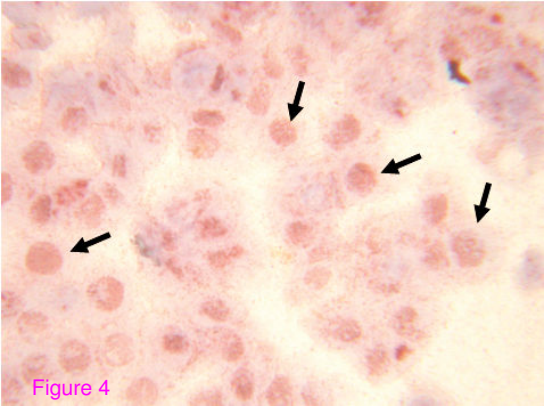


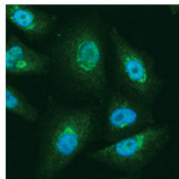
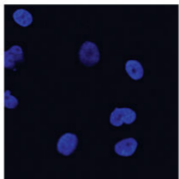
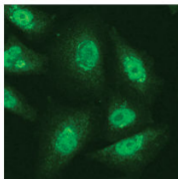
Figure 4

Caspase-14

DAPI

Merge

H838



H1437

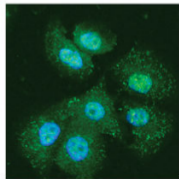
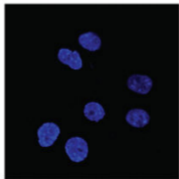
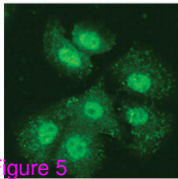


Figure 5

EGFP-caspase-14

Phase contrast

Merge

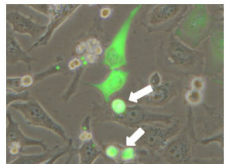
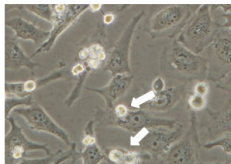
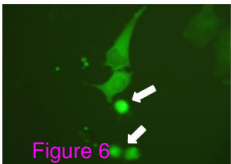
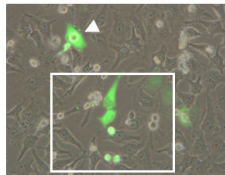
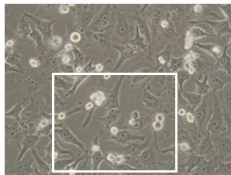
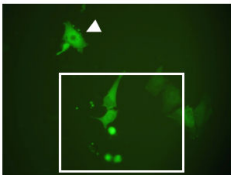


Figure 6

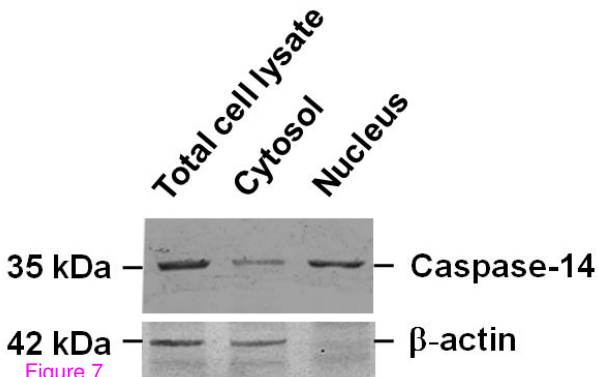
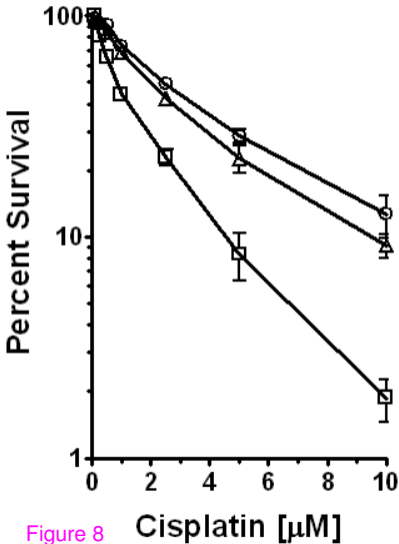


Figure 7



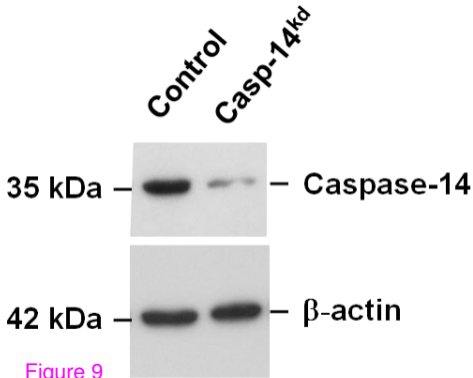


Figure 9

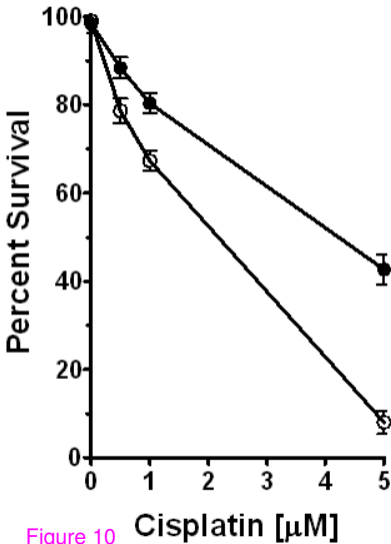


Figure 10

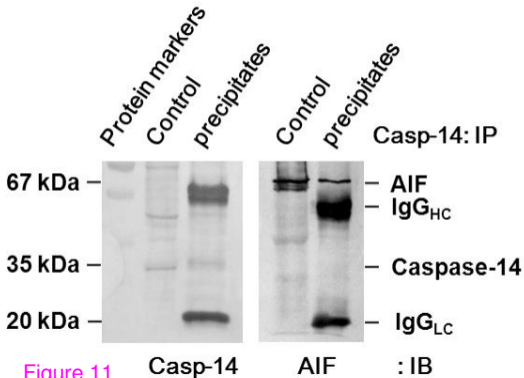


Figure 11

GST
GST-Casp-14
GST-Casp-14-N152
GST-Casp-14- Δ N152

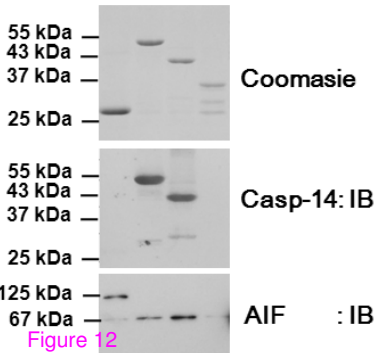


Figure 12

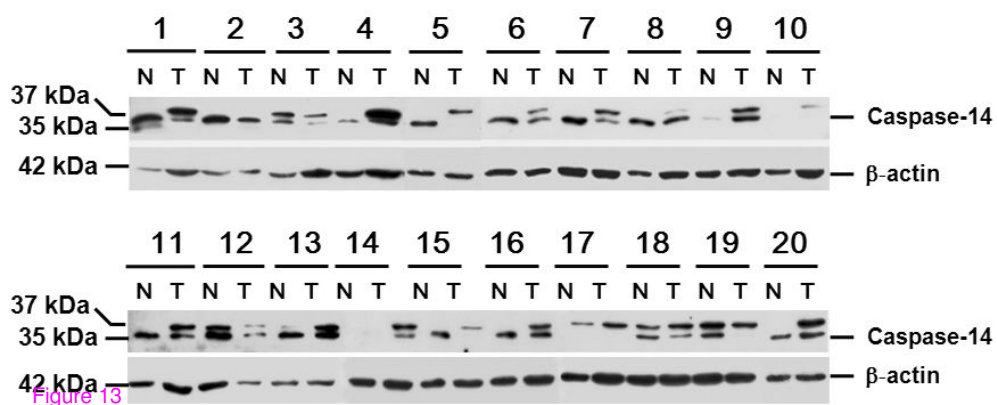
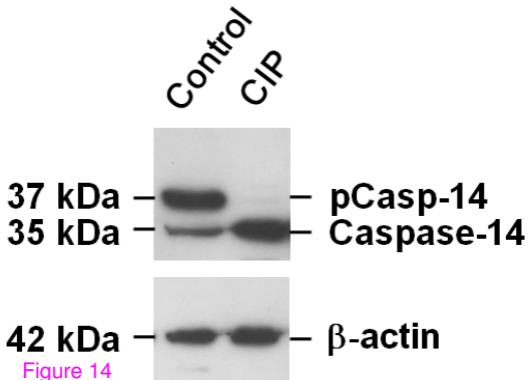
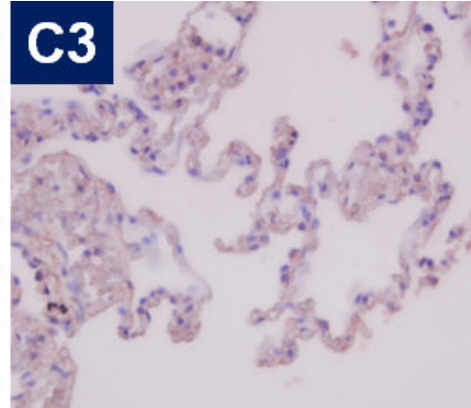
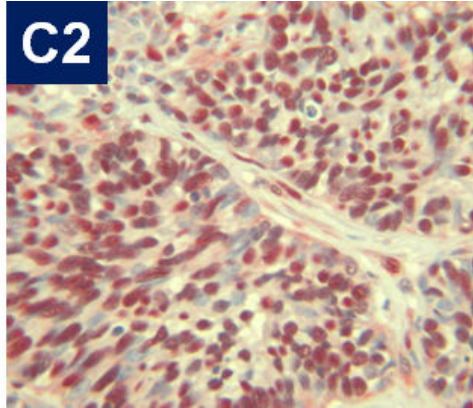
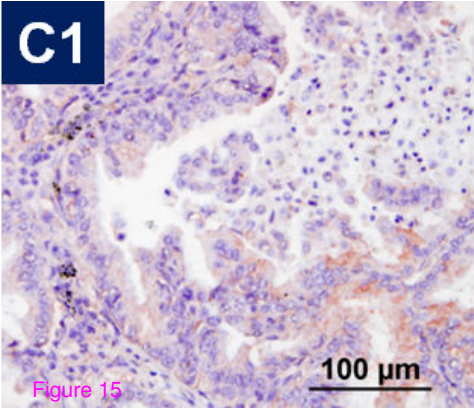


Figure 13





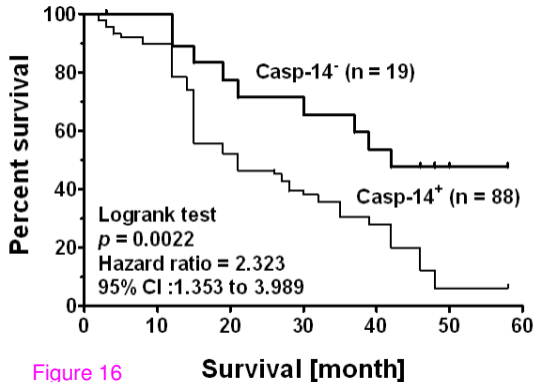


Figure 16

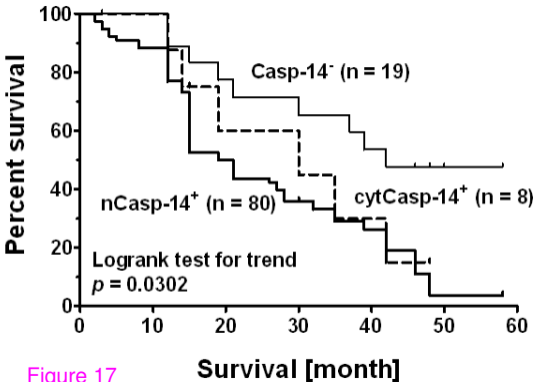


Figure 17

Additional files provided with this submission:

Additional file 1: Supplementary Figures.pdf, 755K

<http://www.molecular-cancer.com/imedia/8603309233591502/supp1.pdf>

Additional file 2: Supplementary Table S1.pdf, 19K

<http://www.molecular-cancer.com/imedia/1379397132359150/supp2.pdf>

Additional file 3: Supplementary Table S2.pdf, 51K

<http://www.molecular-cancer.com/imedia/1600340371359150/supp3.pdf>